Solar Energy Materials & Solar Cells 161 (2017) 368–376

Contents lists available at ScienceDirect

Solar Energy Materials & Solar Cells

journal homepage: www.elsevier.com/locate/solmat

Assessing the stability of high performance solution processed small molecule solar cells

Rongrong Cheacharoen[a], William R. Mateker[a], Qian Zhang[b], Bin Kan[b], Dylan Sarkisian[a], Xiaofeng Liu[c], John A. Love[c], Xiangjian Wan[b], Yongsheng Chen[b], Thuc-Quyen Nguyen[c], Guillermo C. Bazan[c], Michael D. McGehee[a,*]

[a] Department of Materials Science and Engineering, Stanford University, 476 Lomita Mall McCullough Building Stanford, CA 94305, USA
[b] Key Laboratory of Functional Polymer Materials, Collaborative Innovation Center of Chemical Science and Engineering (Tianjin), Center for Nanoscale Science and Technology, Institute of Polymer Chemistry, Nankai University, Wenjin Road 94, Tianjin 300071, China
[c] Center for Polymer and Organic Solids (CPOS), Department of Chemistry & Biochemistry, University of California Santa Barbara, 2520A Physical Sciences Building North, Santa Barbara, CA 93106-5090, USA

ARTICLE INFO

Keywords:
Organic solar cells
Photovoltaic devices
Thermal stability
Photo stability
Solution processed small molecules
Lifetime

ABSTRACT

Solution-processed small molecule-fullerene bulk heterojunction (SM BHJ) solar cells now have power conversion efficiency (PCE) greater than 10%. However, degradation of SM BHJ solar cells has not been well studied. This work reports the first stability study of six high performance molecules including the record SM BHJ solar cells under device operating conditions. Solar cells with a range of donor molecular weight from 1200 to 2300 Da giving 6–10% PCE are monitored in nitrogen gas under 1 sun illumination with maximum power point tracking as well as at 25 °C and 70 °C in the dark. Both heat and light contribute to initial exponential decay or burn-in with total reduction in efficiency from 31% to 66%. Larger molecules are found to be resistant to heat induced burn-in, while more crystalline active layers are more resistant to light induced burn-in. After burn-in, the linear degradation is observed to be governed by thermal processes. Stabilized TS80 lifetimes of the SM BHJ solar cells range from 3450 h to 5600 h. Molecular design towards higher stability should aim at increasing thermal stability while maintaining crystallinity for photostability.

1. Introduction

While organic photovoltaics (OPV) have traditionally utilized semiconducting polymer materials, over the past several years there has been a growing interest in monodisperse small molecules. Compared to polymers, solution processed small molecules are easier to purify and could be more stable with a well-defined molecular weight (MW) [1,2]. When molecules are blended with fullerenes in the bulk heterojunction (BHJ) active layers of a solar cell, the power conversion efficiency (PCE) can now reach over 10% [3–9]. With these promising traits of the molecules, the operating stability remains a critical missing piece of information for projecting practical implementation against competing technologies [10,11].

The degradation mechanisms of polymer solar cells (PSCs) are reasonably well understood and provide background for degradation of solution-processed small molecule bulk heterojunction (SM BHJ) solar cells because both active layers use fullerene and have a BHJ structure. Two regimes of degradation are usually found in OPV: an initial exponential burn-in followed by a slower linear degradation [10]. There are two definitions of lifetime: T80 lifetime and TS80 stabilized lifetime. T80 lifetime is defined by the time it takes a solar cell to degrade to 80% of its initial PCE, which could be within the exponential burn-in period since OPV could burn-in more than 20% [12,13]. On the other hand, TS80 stabilized lifetime is defined by the time it takes a solar cell to degrade 80% after it is burned-in [14]. There are five primary stresses that have been identified to shorten the lifetime of organic solar cells: oxygen, moisture, heat, UV light and visible-near infrared light [11,15–19]. In air, a crystalline and dense neat polymer film photo-oxidizes and bleaches more slowly than an amorphous film of the same material because the molecules are confined and are less able to undergo chemical reactions [15,20]. With a UV filter and encapsulation to remove oxygen and moisture, a polymer solar cell can have a TS80 lifetime of 20 years [13]. In encapsulated PSCs, thermal degradation occurs around a glass transition temperature, above which

* Corresponding author.
E-mail addresses: rrcheacharoen@gmail.com (R. Cheacharoen), wmateker@gmail.com (W.R. Mateker), zhangqian0781@mail.nankai.edu.cn (Q. Zhang), kanbin@mail.nankai.edu.cn (B. Kan), dsarkis@stanford.edu (D. Sarkisian), xiaoflew@gmail.com (X. Liu), jacklove1212@gmail.com (J.A. Love), xjwan@nankai.edu.cn (X. Wan), yschen99@nankai.edu.cn (Y. Chen), quyen@chem.ucsb.edu (T.-Q. Nguyen), bazan@chem.ucsb.edu (G.C. Bazan), mmcgehee@stanford.edu (M.D. McGehee).

http://dx.doi.org/10.1016/j.solmat.2016.12.021
Received 26 July 2016; Received in revised form 7 November 2016; Accepted 10 December 2016

the polymer and fullerene can move and form a blocking layer at an interface, causing the FF to drop [21,22]. Photo degradation in encapsulated PSCs can occur within the active layer due to photochemical processes, causing an open circuit voltage (V_{oc}) loss, [19,23] but are suppressed in PSCs with ordered active layers [24,25]. Fullerene dimerization has also been observed when PSCs with $PC_{60}BM$ are aged under light, [26–29] which results in J_{sc} loss; this effect is particularly enhanced in strongly phase separated systems with pure polymer and fullerene domains [27,28].

While extensive lifetime testing has been performed on PSCs, lifetime tests have been limited to dark storage stability in SM BHJ solar cells [4,30,31]. The lifetime under real operating conditions has not yet been measured. The goals of this study are to report for the first time both the extent of degradation of top performance SM BHJ solar cells aged under real operating conditions and provide guidelines for designing next generation small molecules for thermally and photo stable solar cells.

We have investigated the degradation of six of the highest performing SM BHJ solar cells that were available when this project began. They have PCE ranging from 6% to 10%.[3,6,7,32,33]. The molecules can be divided into two groups of similar chemical structures, as shown in Fig. 1. T1, X2 and F3 have alternating Si-cyclopentadithiophene and benzothiadiazole cores with alkyl-bithiophene endcaps, while DRCN5T, DRCN7T, and DR3TSBDT or the “DR family” have oligothiophene and dialkylthiol-substituted benzodithiophene cores and rhodanine endcaps. Table 1 shows each solar cell stack and its initial performance. We avoid UV, oxygen, and moisture since they are well known to make the organic materials degrade and can be avoided with suitable packaging.[13] We study the effect of visible-near infrared light and heat at 70 °C, the operating temperature,[34,35] on degradation of SM BHJ solar cells beyond 3000 h. We investigate and decouple the effects of dark storage in N_2, thermal and photo degradation, which all can play a role in performance decline. We use grazing incident X-ray diffraction (GIXRD) to characterize the morphology of optimized SM BHJ blend films and neat small molecule thin films that have been aged thermally.

2. Materials and methods

2.1. Solar cell preparation

All solar cells were made on ITO-patterned glass substrates (15 Ω/square, Xinyan Technologies LTD).

2.1.1. Substrate cleaning

Substrates for solar cells were first scrubbed with 1:10 dilute Extran 300 detergent: De-ionized (DI) water, then ultrasonicated in the same solution for 15 min. After, they were rinsed in DI water five times and ultrasonicated in acetone and isopropyl alcohol baths for 15 min each. Finally, the substrates were blown dry with nitrogen gas and placed in a covered petri dish in an oven (95 °C) overnight to remove any residual solvent.

2.1.2. T1 solar cells fabrication

ITO-coated glass substrates were removed from the oven and treated with UV-Ozone plasma for 15 min. Then a PEDOT: PSS solution (Clevious PVP AI 4083) was spun onto the substrates in ambient atmosphere and baked at 140 °C for 10 min, which resulted in a film thickness of about 30 nm. The substrates were quickly transferred into a glovebox with < 10 ppm oxygen and < 10 ppm moisture for active layer deposition. The T1:$PC_{70}BM$ solution with 3:2 weight ratio and 0.4% diiodooctane by volume with an overall concentration of 35 mg/mL in chlorobenzene was prepared the night before and kept on a stirring hotplate at 90 °C. The solution was filtered and spun at 1750 rpm for a minute at maximum acceleration, which gave a 100-nm-thick active layer. The films were dried on a hotplate at 70 °C for 10 min and then were transferred to a dry glovebox for top electrode deposition. 7 nm Ca and 150 nm Al were thermally evaporated one after the other on top of the active layer at a background pressure less than 10^{-6} Torr. The active area of each solar cell device is 0.1 cm^2.

2.1.3. X2 and F3 solar cells fabrication

ITO-coated glass substrates were removed from the oven and transferred directly into a dry glovebox with < 10 ppm oxygen and < 10 ppm moisture. 10 nm MoO_x was thermally evaporated onto the ITO at a background pressure less than 10^{-6} Torr. The substrates were then transferred into a solvent glovebox, with the same level of oxygen and moisture as the previous glovebox, for active layer deposition without any exposure to ambient atmosphere. The active layer solutions of X2:$PC_{60}BM$ and F3:$PC_{60}BM$ with 1:1 weight ratio with an overall concentration of 20 mg/mL in chloroform solution were prepared and kept on a stirring hotplate at 55 °C the night before. The hotplate temperature was brought down to 25 °C just before active layer spinning with the hotplate still stirring. The active layer solution was spun at 2000 rpm for 40 s at 1500 rpm per second acceleration, which both yielded 100 nm thickness. The substrates were then transferred back to the dry glovebox for top electrode deposition. 7 nm Ca and 150 nm Al were thermally evaporated one after the other on top of the active layer at a background pressure less than 1×10^{-6} Torr. The active area of each solar cell device is 0.1 cm^2.

2.1.4. DRCN5T, DRCN7T, and DR3TSBDT solar cells fabrication

DRCN5T, DRCN7T, and DR3TSBDT solar cells were made at Nankai University and completed at Stanford University. ITO-coated

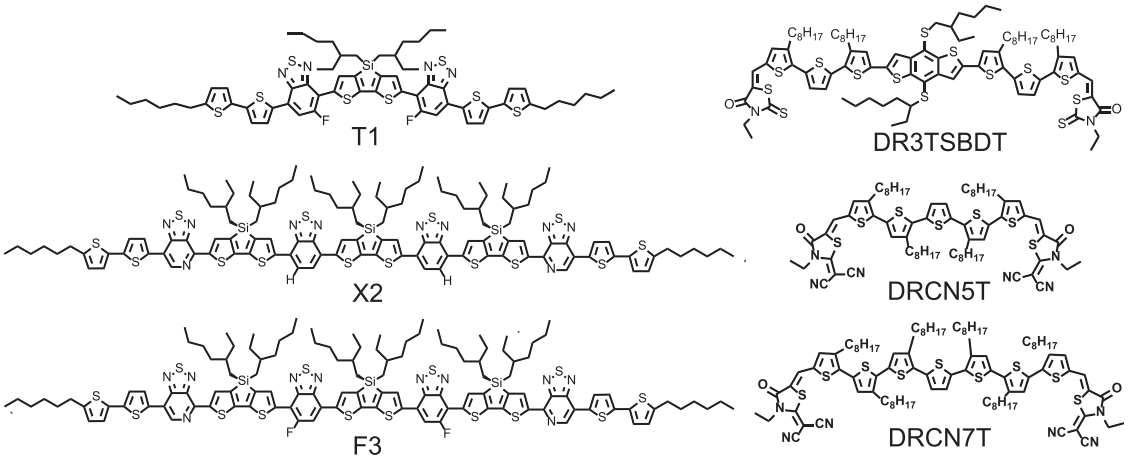

Fig. 1. Chemical structure of solution processed small molecules.

Table 1
SM BHJ solar cell structure and its corresponding average initial J_{sc}, V_{oc}, FF, and PCE values.

Solar Cell Stack	J_{sc} (mA/cm^2)	V_{oc} (V)	FF	PCE
ITO/MoOx/**X2**:PC61BM/Ca/Al	15.6 ± 1.6	0.71 ± 0.02	0.58 ± 0.05	6.3 ± 0.8
ITO/MoOx/**F3**:PC61BM/Ca/Al	13.6 ± 0.4	0.73 ± 0.01	0.73 ± 0.01	7.3 ± 0.2
ITO/PEDOT: PSS/**T1**:PC71BM/Ca/Al	14.4 ± 0.6	0.79 ± 0.01	0.67 ± 0.02	7.6 ± 0.3
ITO/PEDOT: PSS/**DRCN7T**:PC71BM/PFN/Al[6]	14.8 ± 0.1	0.9 ± 0.01	0.68 ± 0.01	9.1 ± 0.3
ITO/PEDOT: PSS/**DR3TSBDT**:PC71BM/ETL–1/Al[3]	14.5 ± 0.2	0.91 ± 0.01	0.73 ± 0.01	9.6 ± 0.4
ITO/PEDOT: PSS/**DRCN5T**:PC71BM/PFN/Al[7]	15.7 ± 0.2	0.92 ± 0.01	0.68 ± 0.01	9.8 ± 0.3

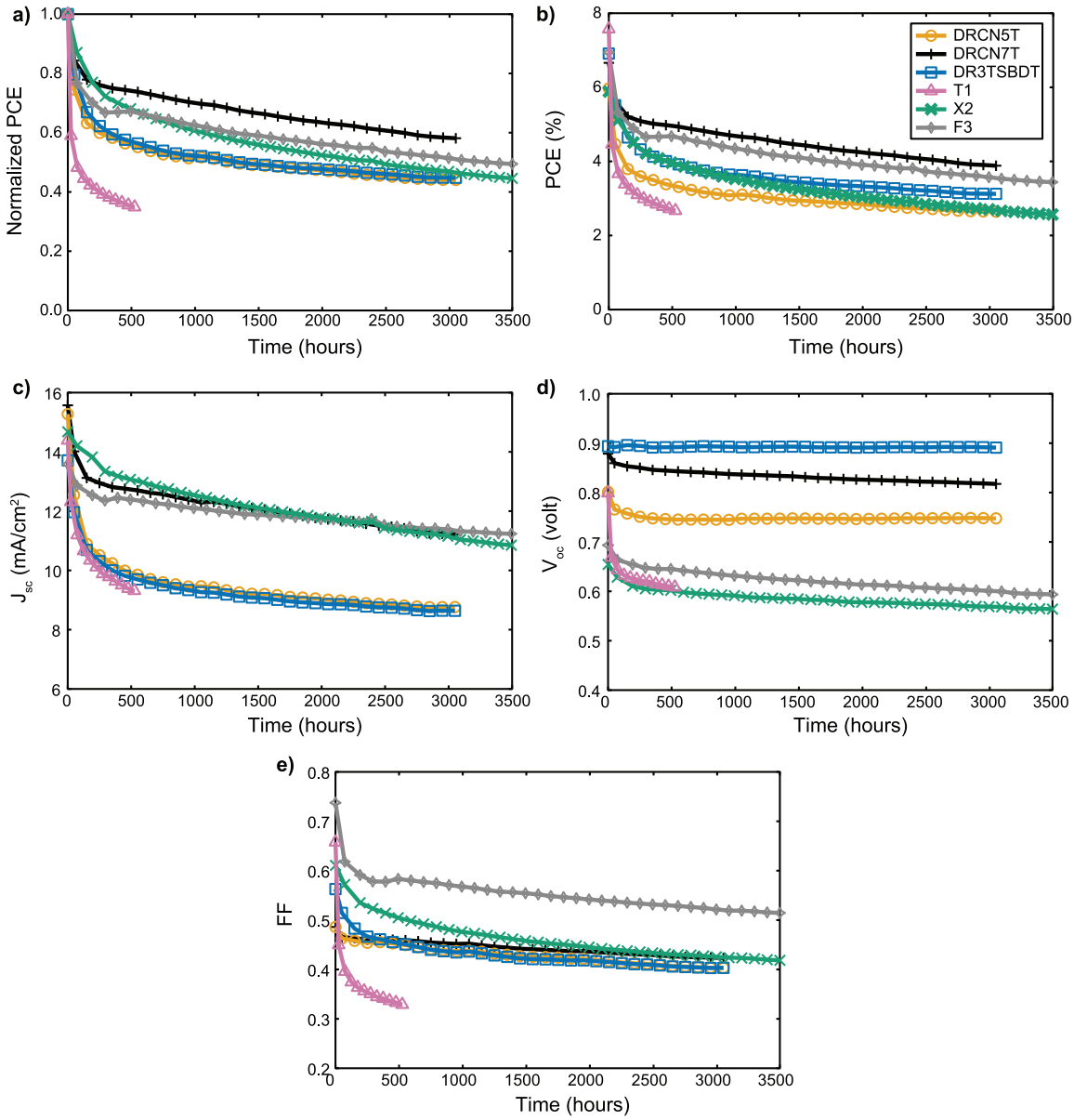

Fig. 2. (a) Normalized PCE vs. aging time for a direct comparison of percent PCE loss among SM BHJ solar cells: (b)-(e) Four figures of merit of SM BHJ solar cells vs. aging time. Burn-in occurs during the first 800–1500 h. All the solar cells were held at the maximum power point under 1 sun simulator inside a controlled environmental chamber with < 0.1 ppm O_2 and < 0.1 ppm moisture.

glass substrates were shipped to Nankai University for charge transporting layers and active layer deposition. ITO-coated glass substrates were cleaned with the same procedure. PEDOT:PSS were spun onto ITO substrate with 3000 rpm and baked at 150 °C for 20 min. The substrates were transferred to an argon-filled glovebox for active layer deposition. The DRCN5T:$PC_{70}BM$ with 1:0.8 weight ratio in a chloroform solution was spin-coated onto the substrates, then thermally annealed at 120 °C for 10 min and cooled to room temperature. The DRCN5T active layer was further placed in a glass covered petri dish containing 150 μL of chloroform for 60 s of solvent vapor annealing, which yielded a 120-nm-thick active layer. The DRCN7T: $PC_{70}BM$ with 1:0.5 weight ratio in chloroform solution was spun onto the substrates. Then the substrates were annealed at 90 °C for 10 min which yielded a 120-nm-thick active layer. Both DRCN5T and DRCN7T active layers had a thin layer of PFN deposited on top under vacuum as an electron transporting layer. The DR3TSBDT:$PC_{70}BM$ with 1:0.8 wt ratio in

Table 2
Burn-in Period, Percentage Burn-in loss, Post burn-in PCE, and TS80 lifetimes of SM BHJ solar cells.

Small Molecule	Burn-in Period (hours)	%Total burn-in Loss	Post burn-in PCE (%)	TS80 lifetime (h)
DR3TSBDT	990	47	3.64	5600
DRCN5T	770	47	3.16	5200
F3	1480	41	4.1	4150
X2	1420	44	3.27	3520
DRCN7T	1160	31	4.62	3450
T1	580	66	2.61	N/A

chloroform solution was spin-coated onto the PEDOT:PSS covered ITO glass substrate, which gave an active layer thickness of 110 nm. The substrates were thermally annealed at 100 °C for 10 min. After that, the substrates were placed in a covered petri dish with 1 μL chloroform for 1 min solvent vapor annealing. The 0.5 mg/mL ETL-1 in methanol solution was then spin coated onto the DR3TSBDT active layer. The vacuum sealed film stacks without top metal electrode were sent back to Stanford University and 250 nm Al was deposited by thermal evaporation at a background pressure of ~10^{-6} Torr. The active area of each solar cell device is 0.1 cm^2.

2.2. Current-voltage characteristic measurement

Current-voltage measurements were carried out inside the glovebox with < 10 ppm oxygen and < 10 ppm moisture. Current-voltage characteristics were recorded using a Keithley 2400 source meter and a Spectra-Physics 91160-1000 solar simulator lamp, which was calibrated to 1 sun (AM 1.5G) with an NREL certified KG-5 filtered silicon photodiode.

2.3. Operating condition aging apparatus/total degradation stability test

Solar cells were loaded into an aluminum chamber with a glass front plate. A copper pipe fed in filtered house nitrogen that had gone through an oxygen scrubber and a desiccant-filled tube and a second copper pipe took the chamber atmosphere out through an oxygen sensor (Alpha Omega Instruments Trace Oxygen Analyzer Series 3000) and a water monitor (Alpha Moisture Systems Model AMT Dewpoint Hygrometer). The atmosphere chamber was vented into the lab via a check valve. The gas flow in and out of the chamber through copper pipes was kept continuous throughout the experiment. For the duration of the experiment, the oxygen was kept below the detection limit of the equipment (< 0.1 ppm) and the water content was around a dew point of −97 °C (< 0.1 ppm). Science Wares Inc. customized electronics to individually control and monitor the solar cell. The aging apparatus operated through a LabVIEW interface that dynamically held each solar cell at maximum power point and graphically recorded the current-voltage curve every hour for all testing duration. The sulfur plasma lamp light source was obtained from LG (6,000 K) and has a good spectral match to AM 1.5 solar spectrum in the visible and little power in the UV (Fig. S1). To account for different spectra overlap between the EQE of each SM BHJ solar cell to sulfur plasma lamp and AM 1.5 solar spectrum, an estimated mismatch factor was obtained by calculating the ratios of J_{sc} measured under an AM 1.5G solar simulator just before loading the chamber vs. J_{sc} measured under the sulfur plasma lamp (Fig. S2 and Table S1). These factors were applied to J_{sc} and PCE data obtained hourly in Fig. 2. A ReflecTech Mirror film, which was laminated onto a plastic sheet, was shaped into a conical reflector to create one-sun homogeneous light intensity among the substrates. The light intensity was monitored using an NREL-calibrated KG-5 filtered silicon photodiode and was kept within 5% of one sun throughout the experiment. The operating condition test in this study refers to the solar cells aged inside the encapsulated aging apparatus under the condition as described above. The temperature of the solar cells under the lamp is around 60–70 °C.

Each solar cell in this study followed an optimal layer combination and fabrication procedure to yield the highest PCE. Table 1 shows each solar cell stack and its initial performance. There were at least five different solar cell substrates for each type of SM BHJ in the test. Apart from T1 solar cells, which were stop being monitored after 500 h because most of the solar cells degraded by more than 60% of the initial PCE, the rest of the SM BHJ solar cells were monitored up to 3000 h.

2.4. Dark storage in N_2 and thermal degradation stability test

The solar cells were kept inside a glovebox (< 10 ppm Oxygen and < 10 ppm moisture) at 25 °C for the “dark storage in N_2 stability test” and placed on top of a 70 °C hotplate, a comparable temperature that the solar cells experience under illumination, for the “thermal stability test.” J-V curves were measured periodically inside the glovebox. Two to three different solar cell substrates and at least three different solar cell substrates for each type of SM BHJ were used in dark storage in N_2 stability and thermal stability test, respectively. Dark storage stability of the DR family SM BHJ solar cells were carried out at Nankai University in the first 0–7 days. After that, the dark storage stability data were collected at Stanford University. The PCEs of the DR family SM BHJ solar cells measured at Nankai University agree with the values at Stanford University on the 7th day of dark storage stability testing ensuring the validity of patching data collected at both institutes.

2.5. Calculating period of burn-in and lifetime in years of SM BHJ solar cells

The burn-in period was found by finding a point where the linear degradation slope becomes constant within 3% Chi-square of the normalized degradation curve in Fig. 2a. The stabilized TS80 lifetime of the organic solar cells is defined as the time from when the linear degradation starts to when the PCE drops by 20% [14]. Taking the slope of the linear degradation, the stabilized TS80 lifetime in hours of all the SM BHJ solar cells were calculated.

2.6. GIXRD measurement of thin films

GIXRD measurements were carried out to characterize the morphology of the initial SM BHJ blend films and neat small molecule films. The neat and blend solutions were deposited onto a piece of a silicon wafer by spin coating inside a nitrogen glovebox. The neat films were stored at 25 °C and aged on a 70 °C hotplate inside a nitrogen glovebox for 120 h. GIXRD measurements were performed at the Stanford Synchrotron Radiation Lightsource, Beamline 11-3 with a photon wavelength of 0.09758 nm and an incident angle of 0.12°. GIXRD images were analyzed using the WxDiff software package.

2.7. Differential scanning calorimetry (DSC)

In order to obtain glass transition temperature (Tg), 3–4 mg of each small molecule donor was measured in TA instrument DSC (Model Q-20 with RCS90) with a heating/cooling ramp rate of 10 °C/min under a nitrogen atmosphere. All the samples were pre-heated beyond their melting temperatures to eliminate their thermal history before monitoring possible thermal transitions.

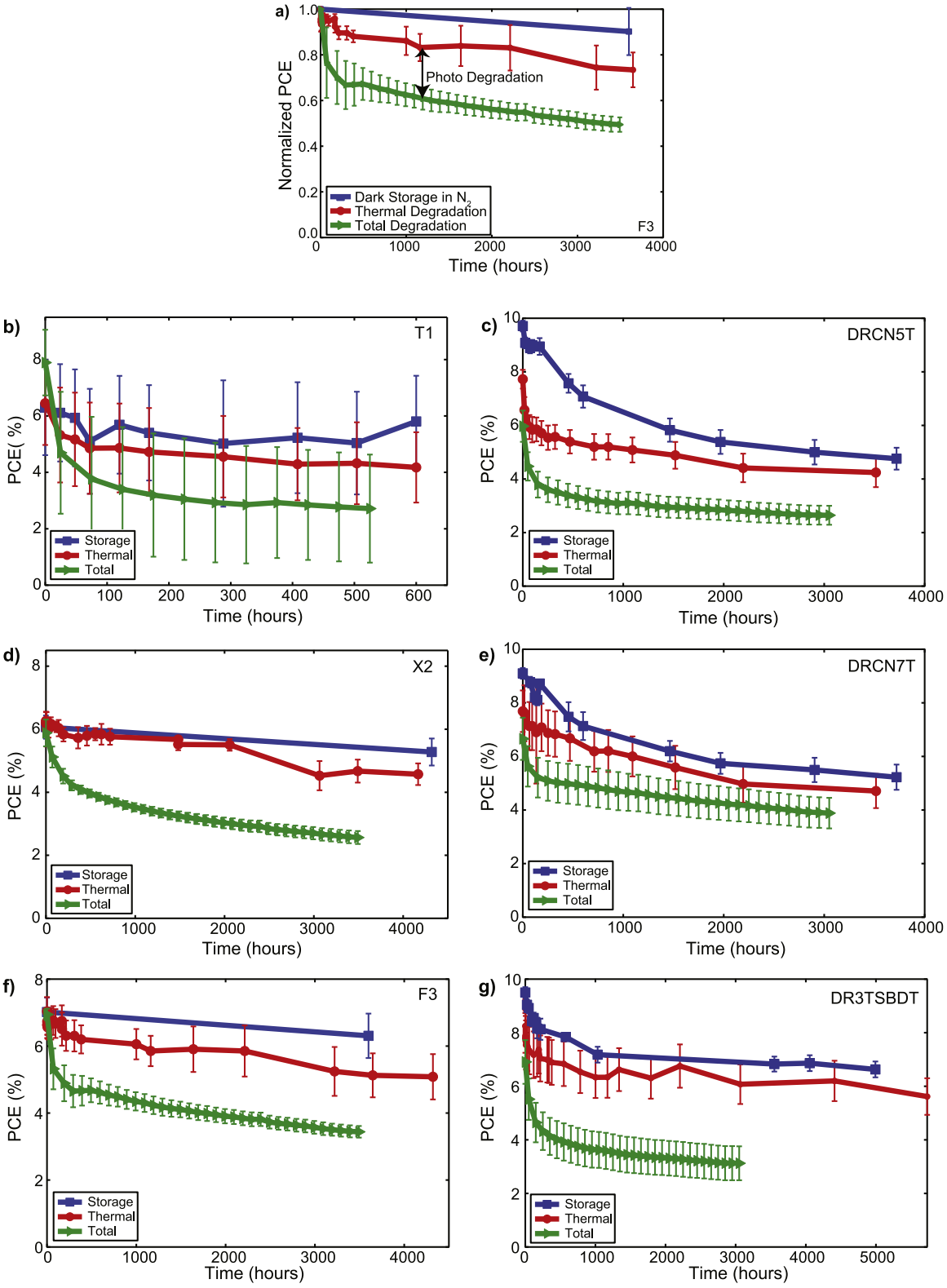

Fig. 3. (a) Normalized degradation of F3 solar cells as a representation to show the definitions of dark storage in N_2 or "storage", thermal, and total degradation and how photodegradation is calculated. (b)-(g) PCE vs. aging time of all six SM BHJ solar cells in this study. Each total degradation datum point represents the PCE averaged every 100 h except those for T1, which were averaged every 50 h. The error bars present standard deviations of at least three devices averaged for each study.

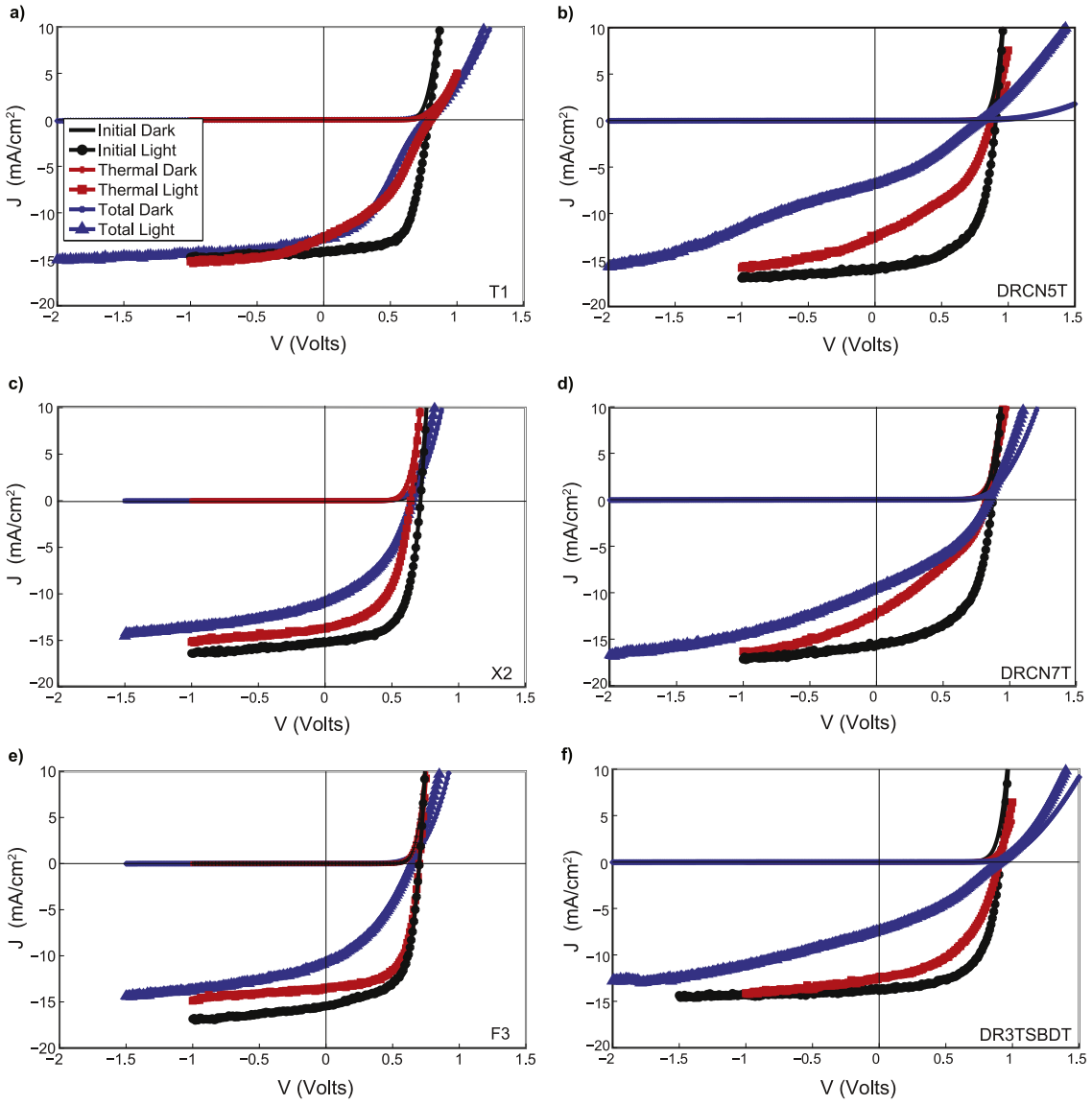

Fig. 4. Current-voltage plots of SM BHJ solar cells (a) T1 (b)DRCN5T (c)X2 (d)DRCN7T (e)F3 (f)DR3TSBDT. Each plot shows the initial, thermal degradation, and total degradation after aging for 3000 h except for T1 solar cells, which were only aged for 500 h.

3. Results and discussion

3.1. Total degradation profile and lifetime of solution processed small molecule solar cells

For all SM BHJ solar cells monitored under operating condition, there are two degradation time periods. In the first thousand hours, the efficiencies of the solar cells exponentially decay by 30–60% (Fig. 2a). Fig. 2b shows that the solar cells with a high initial PCE and a small burn-in can have high post burn-in PCE, such as DRCN7T. Some loss in performance of the DR family SM BHJ solar cells is observed while setting up the lifetime testing chamber resulting in a lower starting efficiency (Fig. 2b). All SM BHJ solar cells finish burning-in after 800–1500 h. The efficiency losses during burn-in vary from 31–66% (Table 2), which is similar to burn-in loss in polymer solar cells. [13,14] The loss in J_{sc} and FF are the two biggest causes of burn-in deterioration shown in Fig. 2c-e.

After burn-in, the degradation slows down as the PCE flattens out into a linear decay. Linear degradation is mostly contributed by loss in FF since the slopes in Fig. 2e (FF) and 2b (PCE) are similar. The stabilized TS80 lifetimes of SM BHJ solar cells extracted from the degradation profile range from 3450 to 5600 h as reported in Table 2. To get a better understanding of how heat and light contribute to the burn-in and linear degradation, thermal and photo degradation need to be decoupled.

3.2. Comparing degradation with thermal, photo, and no stress

In parallel with testing total degradation of SM BHJ solar cells under illumination, we monitored two additional stability tests in the dark inert atmosphere: “dark storage in N_2” and thermal stability. Fig. 3a shows how each degradation term is defined and calculated. Fig. 3b-g show degradation of the PCEs from all three stability tests for each SM BHJ solar cell.

Similar to total degradation, there is a burn-in period followed by a linear degradation in both thermal and dark storage in N_2 stability tests. Most of the degradation in the dark occurs under storage, which leads to reduced efficiency between fresh solar cells and the beginning of the lifetime testing. Burn-in degradation in the dark is less than total burn-in, which indicates a contribution from photo-induced processes. Past burn-in, however, the slopes of total and thermal degradation are the same. This observation suggests that the stabilized TS80 lifetime of

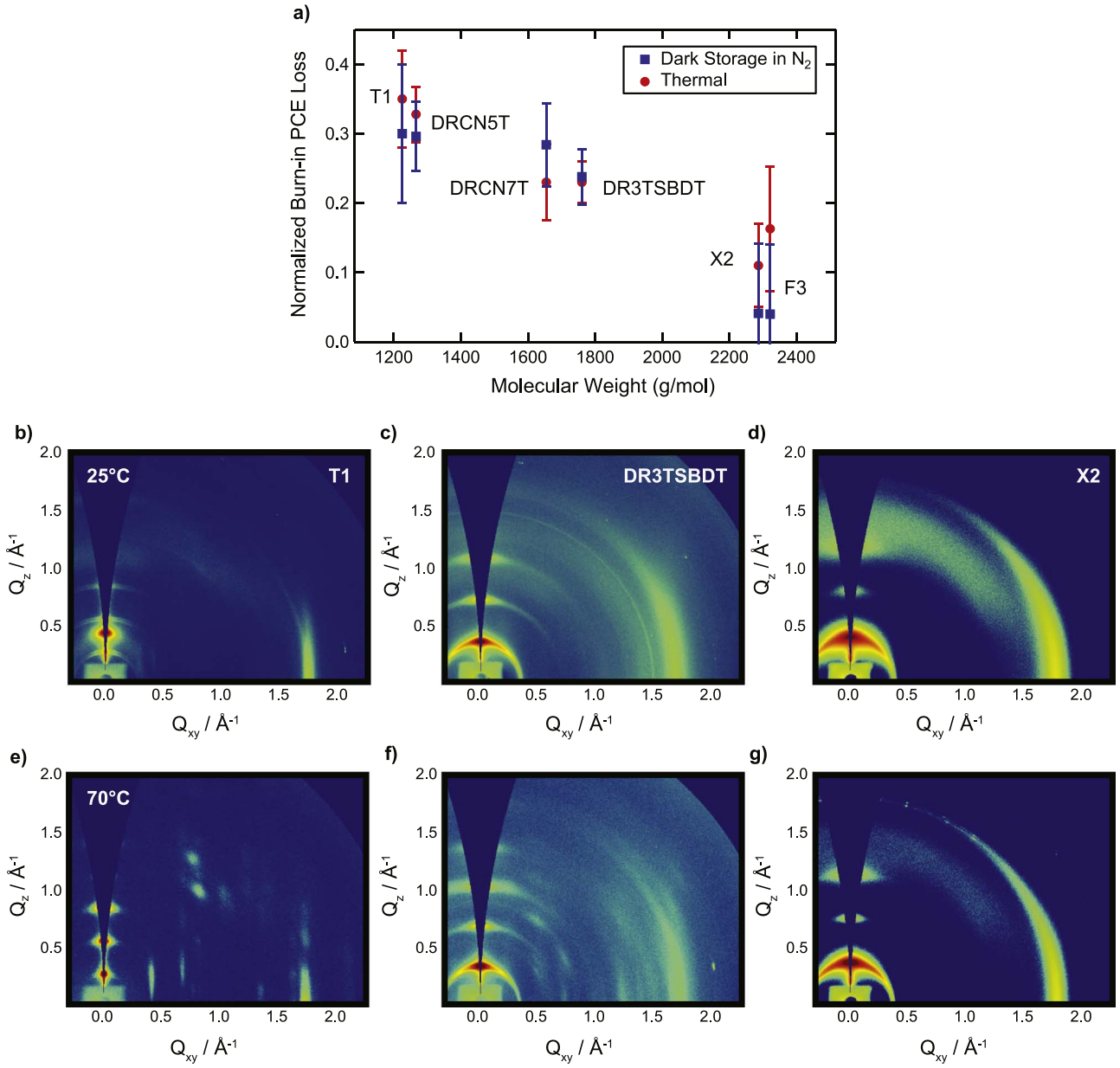

Fig. 5. (a) Normalized burn-in degradation in the dark of SM BHJ solar cells stored at 25 °C and aged at 70 °C in the glovebox (< 10 ppm O_2 and < 1 ppm moisture) (b)-(d) neat film of T1, DR3TSBDT, and X2 stored in the dark in N_2 for 120 h (e)-(g) neat film of T1, DR3TSBDT, and X2 aged at 70 °C for 120 h. Burn-in period is defined by total degradation curve in Fig. 2.

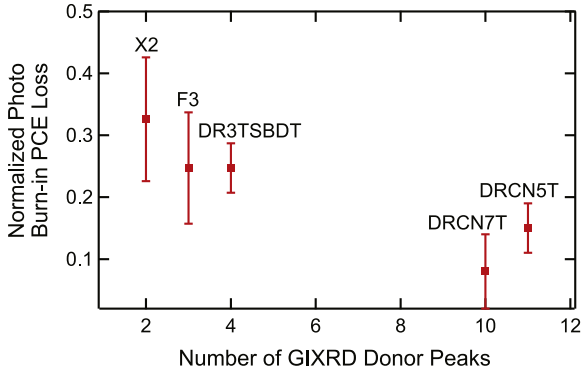

Fig. 6. Normalized photo burn-in efficiency loss vs. number of donor GIXRD peaks in each solution processed small molecule: fullerene optimized blend film.

the SM BHJ solar cells is limited by thermal degradation.

The current-voltage (J-V) curves of fresh and aged devices are plotted in Fig. 4. In all cases most of the loss for both thermal and total degradation is in FF and J_{sc}. Fill factor loss is most likely coming from a reduced charge carrier mobility in the donor materials [36].

An s-shaped J-V curve with unusually small fill factor is found in the T1 and the DR family of SM BHJ solar cells after aging (Fig. 4a, b, d, and f). The current in these cells can be recovered by operating in far reverse bias, which suggests that there is either a charge transport or charge extraction problem that causes the J_{sc} loss and lowers the FF [2,22]. By simply peeling off the top metal electrode and evaporating a new top electrode onto degraded T1 solar cells, we could recover the original J_{sc} and FF (Fig. S3). We have seen this behavior before in polymer solar cells and shown that it arises when donor molecules are able to diffuse to the electrode and stick to it [22], thereby creating a charge extraction barrier. It is interesting that the two smallest molecules are the ones that seem to move around in the film and cause problems. We further explore how thermal degradation depends

on molecular weight in the next section.

In X2 and F3 SM BHJ solar cells, there is no S-shape in the J-V curve after aging (Fig. 4c and e). Part of the J_{sc} and FF degradation is thermally induced, which most likely contributes to degradation in the bulk as we observed no extraction barrier in J-V curve. The other part of the loss is likely due to light-induced fullerene dimerization. Fullerene dimerization occurs more in polymer solar cells with PC60BM than PC70BM, resulting in J_{sc} and FF loss [27,28]. X2 and F3 have been shown to have minimal mixing with pure fullerene phase [37], therefore it is likely that fullerene dimerization would occur in these systems.

3.3. Thermal degradation as a function of molecule size

Fig. 5a plots the amount of thermal degradation that occurred during burn-in in the dark at 25 °C and 70 °C versus the molecular weight of the six donor molecules. The lower MW molecules clearly suffer from thermal degradation more than those of higher MW. The MW of a molecule could be related to its ability to rearrange within the film, with smaller molecules more readily able to move and change the local morphology in different regions of the film. We attempted to measure the glass transition temperature of all of the materials in this study using differential scanning calorimetry, but unfortunately did not observe any clear glass transitions and found this experiment to be ineffective for assessing which molecules are the most mobile in the relevant temperature range. (Fig. S4) It is often difficult to determine the glass transition temperature of conjugated molecules and there have been examples where the reported values vary by over 100 °C. For this reason we are choosing not to attempt to extract a number that might not be accurate. We think the best way to predict whether or not molecules will stay in place over a long period of time at a certain temperature is to study thermal degradation over a period of weeks at 70 °C or "a slightly higher temperature for a shorter period of time."

The appearance of new peaks in thermally aged neat thin films of T1, DR3TSBDT, and X2 was monitored and compared with films kept at 25 °C using GIXRD. Low MW films get more ordered at elevated temperature, with new peaks observed in Fig. 5e and f, while higher MW films barely change (Fig. 5g.) An increase in molecular ordering with heat could result in bulk morphology diverging from its optimum or morphological degradation at an interface, either of which could cause FF loss in the solar cells. One example of a bulk morphology change is the phase separation of the small molecule and fullerenes in the SM BHJ blend, which would result in the formation of larger pure phase crystallites. Such crystallites lower J_{sc} and FF in some SM BHJ solar cell systems [38,39]. On the other hand, molecular rearrangement around the active layer/transporting layer interface could result in a transport blocking layer, which has been shown to reduce FF in PSCs with low Tg [22]. All these possibilities could explain why the low MW donor SM BHJ solar cells burn-in in the dark more than the heavier MW SM BHJ solar cells in Fig. 5a. Along with using heavier MW small molecules for thermal stability, crosslinking, which has been shown to improve morphological stability in PSCs, could also reduce thermal burn-in in SM BHJ solar cells [40–45].

3.4. Photo induced burn-in

The amount of photodegradation is quantified by taking the difference between total and thermal degradation in Fig. 3a. Previous studies of degradation in PSCs have shown that more crystalline solar cells experience less photo-induced burn-in [15,20,24,46–50]. To see if this trend holds for the molecules in this study, we normalized the photoinduced burn-in and plotted it versus the number of donor diffraction peaks in the six blend films (Fig. 6). More details describing peak counting from GIXRD plots can be found in Fig. S5. T1 solar cell data are not included in this plot because the large error bars in both total and thermal degradation make it hard to quantify photo-induced burn-in. Fig. 6 shows that SM BHJ solar cells photo burn-in from 8% to 33% of the original PCE. As expected, solar cells with a large number of donor diffraction peaks burn-in less.

On top of having the least ordered active layer morphology, fullerene dimerization could add to high photodegradation of X2 and F3 SM BHJ solar cells, which are the only two solar cells using $PC_{60}BM$ in this study [27,51]. Removing these two SM BHJ solar cells from the graph, the photo stability trend in more ordered blend film is still clear.

4. Conclusions

The rapid increase in recorded efficiencies for OPV solar cells is encouraging for their potential use as an alternative energy source. However, for solution-processed small molecule BHJ solar cells to become a commercially relevant technology, they must first demonstrate long-term stability. This work reports the first comparative study of long-term stability data for six of the highest performing SM BHJ solar cells. We observed both thermal and photoinduced degradation.

For the rate of progress towards stabilizing organic solar cells to be maximized, it is important to speed up the rate at which materials are tested. We typically do not see indications of a glass transition in DSC curves of solution-processed small molecule. Instead of measuring the Tg, we encourage chemists who are developing new molecules for solar cells to measure the efficiency of their solar cells before and after one day on a hot plate at 80 °C. If substantial degradation occurs, we urge them to take measures to improve the thermal stability, such as increasing molecular weight, cross-linking, and using stiffer molecules. If the organic solar cell community starts measuring and reporting stability metrics as it routinely does for efficiency metrics, there is a higher chance for our community to develop stable materials that can be processed inexpensively. Research groups with specialized equipment for performing long-term stability tests will be more likely to find highly stable materials if this prescreening is performed by as many chemistry groups as possible and detailed studies are reserved for the most promising molecules.

Acknowledgement

This work was supported by the Office of Naval Research (ONR Award No. N000141410280) and Ministry of Science and Technology, Royal Thai Government. We thank LG for providing the sulfur plasma lamps. We also would like to thank Dr. Stefan Oosterhout for his help with a GIXRD measurement.

Appendix A. Supporting information

Supplementary data associated with this article can be found in the online version at doi:10.1016/j.solmat.2016.12.021.

References

[1] J. Kong, S. Song, M. Yoo, G.Y. Lee, O. Kwon, J.K. Park, et al., Long-term stable polymer solar cells with significantly reduced burn-in loss, Nat. Commun. 5 (2014) 5688. http://dx.doi.org/10.1038/ncomms6688.
[2] W.R. Mateker, J.D. Douglas, C. Cabanetos, I.T. Sachs-Quintana, J.A. Bartelt, E.T. Hoke, et al., Improving the long-term stability of PBDTTPD polymer solar cells through material purification aimed at removing organic impurities, Energy Environ. Sci. 6 (2013) 2529. http://dx.doi.org/10.1039/c3ee41328d.
[3] B. Kan, Q. Zhang, M. Li, X. Wan, W. Ni, G. Long, et al., Solution-processed organic solar cells based on dialkylthiol-substituted benzodithiophene unit with efficiency near 10%, J. Am. Chem. Soc. 136 (2014) 15529–15532. http://dx.doi.org/10.1021/ja509703k.
[4] K. Sun, Z. Xiao, S. Lu, W. Zajaczkowski, W. Pisula, E. Hanssen, et al., A molecular nematic liquid crystalline material for high-performance organic photovoltaics, Nat. Commun. 6 (2015) 6013. http://dx.doi.org/10.1038/ncomms7013.
[5] Y. Liu, C.-C. Chen, Z. Hong, J. Gao, Y.M. Yang, H. Zhou, et al., Solution-processed small-molecule solar cells: breaking the 10% power conversion efficiency, Sci. Rep. 3 (2013) 3356. http://dx.doi.org/10.1038/srep03356.
[6] Q. Zhang, B. Kan, F. Liu, G. Long, X. Wan, X. Chen, et al., Small-molecule solar cells with efficiency over 9%, Nat. Photonics 9 (2014) 35–41. http://dx.doi.org/

10.1038/nphoton.2014.269.
[7] B. Kan, M. Li, Q. Zhang, F. Liu, X. Wan, Y. Wang, et al., A series of simple oligomer-like small molecules based on oligothiophenes for solution-processed solar cells with high efficiency, J. Am. Chem. Soc. 137 (2015) 3886–3893. http://dx.doi.org/10.1021/jacs.5b00305.
[8] V. Gupta, L.F. Lai, R. Datt, S. Chand, A.J. Heeger, G.C. Bazan, et al., Dithienogermole-based solution-processed molecular solar cells with efficiency over 9%, Chem. Commun. 52 (2016) 8596–8599. http://dx.doi.org/10.1039/C6CC03998G.
[9] J.-L.Wang, K.-K.Liu, J.Yan, Z.Wu, F.Liu, F.Xiao, et al., Series of multifluorine substituted oligomers for organic solar cells with efficiency over 9% and fill factor of 0.77 by combination thermal and solvent vapor annealing, 2016.
[10] M. Jørgensen, K. Norrman, S.A. Gevorgyan, T. Tromholt, B. Andreasen, F.C. Krebs, Stability of polymer solar cells, Adv. Mater. 24 (2012) 580–612. http://dx.doi.org/10.1002/adma.201104187.
[11] N. Grossiord, J.M. Kroon, R. Andriessen, P.W.M. Blom, Degradation mechanisms in organic photovoltaic devices, Org. Electron. 13 (2012) 432–456. http://dx.doi.org/10.1016/j.orgel.2011.11.027.
[12] C.H. Peters, I.T. Sachs-Quintana, W.R. Mateker, T. Heumueller, J. Rivnay, R. Noriega, et al., The mechanism of burn-in loss in a high efficiency polymer solar cell, Adv. Mater. 24 (2012) 663–668 ⟨http://www.ncbi.nlm.nih.gov/pubmed/21989825⟩ (accessed 30.10.15).
[13] W.R. Mateker, I.T. Sachs-Quintana, G.F. Burkhard, R. Cheacharoen, M.D. McGehee, Minimal long-term intrinsic degradation observed in a polymer solar cell illuminated in an oxygen-free environment, Chem. Mater. 27 (2015) 404–407 ⟨http://pubs.acs.org.ezproxy.stanford.edu/doi/abs/10.1021/cm504650a⟩ (accessed 13.10.15).
[14] C.H. Peters, I.T. Sachs-Quintana, J.P. Kastrop, S. Beaupré, M. Leclerc, M.D. McGehee, High efficiency polymer solar cells with long operating lifetimes, Adv. Energy Mater. 1 (2011) 491–494. http://dx.doi.org/10.1002/aenm.201100138.
[15] W.R. Mateker, T. Heumueller, R. Cheacharoen, I.T. Sachs-Quintana, M.D. McGehee, J. Warnan, et al., Molecular packing and arrangement govern the, Chem. Mater. 27 (2015) 6345–6353. http://dx.doi.org/10.1021/acs.chemmater.5b02341.
[16] S.A. Gevorgyan, M.V. Madsen, B. Roth, M. Corazza, M. Hösel, R.R. Søndergaard, et al., Lifetime of organic, Adv. Energy Mater. 6 (2016) 1501208. http://dx.doi.org/10.1002/aenm.201501208.
[17] H.C. Weerasinghe, S.E. Watkins, N. Duffy, D.J. Jones, A.D. Scully, Influence of moisture out-gassing from encapsulant materials on the lifetime of organic solar cells, Sol. Energy Mater. Sol. Cells 132 (2015) 485–491. http://dx.doi.org/10.1016/j.solmat.2014.09.030.
[18] M. Manceau, S. Chambon, A. Rivaton, J.-L. Gardette, S. Guillerez, N. Lemaître, Effects of long-term UV–visible light irradiation in the absence of oxygen on P3HT and P3HT:PCBM blend, Sol. Energy Mater. Sol. Cells 94 (2010) 1572–1577. http://dx.doi.org/10.1016/j.solmat.2010.03.012.
[19] M.O. Reese, A.M. Nardes, B.L. Rupert, R.E. Larsen, D.C. Olson, M.T. Lloyd, et al., Photoinduced degradation of polymer and, Adv. Funct. Mater. 20 (2010) 3476–3483. http://dx.doi.org/10.1002/adfm.201001079.
[20] Y.W. Soon, S. Shoaee, R.S. Ashraf, H. Bronstein, B.C. Schroeder, W. Zhang, et al., Material crystallinity as a determinant of triplet dynamics and oxygen quenching in donor polymers for organic photovoltaic devices, Adv. Funct. Mater. 24 (2014) 1474–1482. http://dx.doi.org/10.1002/adfm.201302612.
[21] B. Song, Q.C. Burlingame, K. Lee, S.R. Forrest, Reliability of mixed-heterojunction organic photovoltaics grown via organic vapor phase deposition, Adv. Energy Mater. 5 (2015) 1401952. http://dx.doi.org/10.1002/aenm.201401952.
[22] I.T. Sachs-Quintana, T. Heumüller, W.R. Mateker, D.E. Orozco, R. Cheacharoen, S. Sweetnam, et al., Electron barrier formation at the, Adv. Funct. Mater. 24 (2014) 3978–3985. http://dx.doi.org/10.1002/adfm.201304166.
[23] I. Fraga Domínguez, P.D. Topham, P.-O. Bussière, D. Bégué, A. Rivaton, Unravelling the photodegradation mechanisms of a low bandgap polymer by combining experimental and modeling approaches, J. Phys. Chem. C 119 (2015) 2166–2176. http://dx.doi.org/10.1021/jp5103065.
[24] T. Heumueller, W.R. Mateker, I.T. Sachs-Quintana, K. Vandewal, J.A. Bartelt, T.M. Burke, et al., Reducing burn-in voltage loss in polymer solar cells by increasing the polymer crystallinity, Energy Environ. Sci. 7 (2014) 2974. http://dx.doi.org/10.1039/C4EE01842G.
[25] T. Heumueller, T.M. Burke, W.R. Mateker, I.T. Sachs-Quintana, K. Vandewal, C.J. Brabec, et al., Disorder-induced, Adv. Energy Mater. 5 (2015) 1500111. http://dx.doi.org/10.1002/aenm.201500111.
[26] F. Piersimoni, G. Degutis, S. Bertho, K. Vandewal, D. Spoltore, T. Vangerven, et al., Influence of fullerene photodimerization on the PCBM crystallization in polymer: fullerene bulk heterojunctions under thermal stress, J. Polym. Sci. B Polym. Phys. 51 (2013) 1209–1214 ⟨http://doi.wiley.com/10.1002/polb.23330⟩ (accessed 23.04.15).
[27] A. Distler, T. Sauermann, H.-J. Egelhaaf, S. Rodman, D. Waller, K.-S. Cheon, et al., The effect of PCBM dimerization on the performance of bulk heterojunction solar cells, Adv. Energy Mater. 4 (2014) 1300693 ⟨http://doi.wiley.com/10.1002/aenm.201300693⟩ (accessed 23.04.15).
[28] T. Heumueller, W.R. Mateker, A. Distler, U.F. Fritze, R. Cheacharoen, W.H. Nguyen, et al., Morphological and electrical control of fullerene dimerization determines organic photovoltaic stability, Energy Environ. Sci. (2016) ⟨http://pubs.rsc.org/en/content/articlehtml/2016/ee/c5ee02912k⟩ (accessed 01.12.15).
[29] N. Wang, X. Tong, Q. Burlingame, J. Yu, S.R. Forrest, Photodegradation of small-molecule organic photovoltaics, Sol. Energy Mater. Sol. Cells 125 (2014) 170–175 ⟨http://www.sciencedirect.com/science/article/pii/S092702481400124X⟩ (accessed 15.12.15).
[30] G. Long, B. Wu, X. Yang, B. Kan, Y.-C. Zhou, L.-C. Chen, et al., Enhancement of performance and mechanism studies of all-solution processed small-molecule based solar cells with an InvertedStructure, ACS Appl. Mater. Interfaces 7 (2015) 21245–21253. http://dx.doi.org/10.1021/acsami.5b05317.
[31] A.K.K. Kyaw, D.H. Wang, V. Gupta, J. Zhang, S. Chand, G.C. Bazan, et al., Efficient solution-processed small-molecule solar cells with inverted structure, Adv. Mater. 25 (2013) 2397–2402. http://dx.doi.org/10.1002/adma.201300295.
[32] T.S. van der Poll, J.A. Love, T.-Q. Nguyen, G.C. Bazan, Non-basic high-performance molecules for solution-processed organic solar cells, Adv. Mater. 24 (2012) 3646–3649. http://dx.doi.org/10.1002/adma.201201127.
[33] X. Liu, Y. Sun, L.A. Perez, W. Wen, M.F. Toney, A.J. Heeger, et al., Narrow-band-gap conjugated chromophores with extended molecular lengths, J. Am. Chem. Soc. 134 (2012) 20609–20612. http://dx.doi.org/10.1021/ja310483w.
[34] M. Koehl, M. Heck, S. Wiesmeier, J. Wirth, Modeling of the nominal operating cell temperature based on outdoor weathering, Sol. Energy Mater. Sol. Cells 95 (2011) 1638–1646 ⟨http://www.sciencedirect.com/science/article/pii/S0927024811000304⟩ (accessed 25.10.13).
[35] A. Rougier, C. Guy, M. Koehl, M. Heck, S. Wiesmeier, Modelling of conditions for accelerated lifetime testing of humidity impact on PV-modules based on monitoring of climatic data, Sol. Energy Mater. Sol. Cells 99 (2012) 282–291 ⟨http://www.sciencedirect.com/science/article/pii/S0927024811006921⟩ (accessed 25.10.13).
[36] J.A. Bartelt, D. Lam, T.M. Burke, S.M. Sweetnam, M.D. McGehee, Charge-carrier mobility requirements for bulk heterojunction solar cells with high fill factor and external quantum efficiency, Adv. Energy Mater. 5 (2015) 1500577. http://dx.doi.org/10.1002/aenm.201500577.
[37] Y. Huang, X. Liu, C. Wang, J.T. Rogers, G.M. Su, M.L. Chabinyc, et al., Structural characterization of a composition tolerant bulk heterojunction blend, Adv. Energy Mater. 4 (2014) 1301886. http://dx.doi.org/10.1002/aenm.201301886.
[38] A. Sharenko, M. Kuik, M.F. Toney, T.-Q. Nguyen, Crystallization-induced phase separation in, Adv. Funct. Mater. 24 (2014) 3543–3550. http://dx.doi.org/10.1002/adfm.201304100.
[39] Y. Sun, G.C. Welch, W.L. Leong, C.J. Takacs, G.C. Bazan, A.J. Heeger, Solution-processed small-molecule solar cells with 6.7% efficiency, Nat. Mater. 11 (2012) 44–48. http://dx.doi.org/10.1038/nmat3160.
[40] A. Tournebize, A. Rivaton, J.-L. Gardette, C. Lombard, B. Pépin-Donat, S. Beaupré, et al., How photoinduced crosslinking under operating conditions can reduce PCDTBT-based solar cell efficiency and then stabilize it, Adv. Energy Mater. 4 (2014) 1301530. http://dx.doi.org/10.1002/aenm.201301530.
[41] B.C. Schroeder, Z. Li, M.A. Brady, G.C. Faria, R.S. Ashraf, C.J. Takacs, et al., Enhancing fullerene-based solar cell lifetimes by addition of a fullerene dumbbell, Angew. Chem. Int. Ed. Engl. 53 (2014) 12870–12875 ⟨http://onlinelibrary.wiley.com/doi/10.1002/anie.201407310/full⟩ (accessed 11.08.15).
[42] G. Wantz, L. Derue, O. Dautel, A. Rivaton, P. Hudhomme, C. Dagron-Lartigau, Stabilizing polymer-based bulk heterojunction solar cells via crosslinking, Polym. Int. 63 (2014) 1346–1361 ⟨http://doi.wiley.com/10.1002/pi.4712⟩ (accessed 11.06.15).
[43] G. Griffini, J.D. Douglas, C. Piliego, T.W. Holcombe, S. Turri, J.M.J. Fréchet, et al., Long-term thermal stability of high-efficiency polymer solar cells based on photocrosslinkable donor-acceptor conjugated polymers, Adv. Mater. 23 (2011) 1660–1664 ⟨http://www.ncbi.nlm.nih.gov/pubmed/21472794⟩ (accessed 16.12.15).
[44] H.J. Kim, A.-R. Han, C.-H. Cho, H. Kang, H.-H. Cho, M.Y. Lee, et al., Solvent-resistant organic transistors and thermally stable organic photovoltaics based on cross-linkable conjugated polymers, Chem. Mater. 24 (2012) 215–221. http://dx.doi.org/10.1021/cm203058p (accessed 16.12.15).
[45] C.-P. Chen, C.-Y. Huang, S.-C. Chuang, Highly thermal stable and efficient organic photovoltaic cells with crosslinked networks appending open-cage fullerenes as additives, Adv. Funct. Mater. 25 (2015) 207–213 ⟨http://doi.wiley.com/10.1002/adfm.201401735⟩ (accessed 16.12.15).
[46] H. Hintz, H.-J. Egelhaaf, L. Lüer, J. Hauch, H. Peisert, T. Chasse, Photodegradation of P3HT–A systematic study of environmental factors, Chem. Mater. 23 (2011) 145–154. http://dx.doi.org/10.1021/cm102373k.
[47] A. Dupuis, P. Wong-Wah-Chung, A. Rivaton, J.-L. Gardette, Influence of the microstructure on the photooxidative degradation of poly(3-hexylthiophene), Polym. Degrad. Stab. 97 (2012) 366–374. http://dx.doi.org/10.1016/j.polymdegradstab.2011.12.012.
[48] A. Tournebize, J.-L. Gardette, C. Taviot-Guého, D. Bégué, M.A. Arnaud, C. Dagron-Lartigau, et al., Is there a photostable conjugated polymer for efficient solar cells?, Polym. Degrad. Stab. 112 (2015) 175–184. http://dx.doi.org/10.1016/j.polymdegradstab.2014.12.018.
[49] A. Rivaton, S. Chambon, M. Manceau, J.-L. Gardette, N. Lemaître, S. Guillerez, Light-induced degradation of the active layer of polymer-based solar cells, Polym. Degrad. Stab. 95 (2010) 278–284. http://dx.doi.org/10.1016/j.polymdegradstab.2009.11.021.
[50] Y.W. Soon, H. Cho, J. Low, H. Bronstein, I. McCulloch, J.R. Durrant, Correlating triplet yield, singlet oxygen generation and photochemical stability in polymer/fullerene blend films, Chem. Commun. (Camb.). 49 (2013) 1291–1293. http://dx.doi.org/10.1039/c2cc38243a.
[51] H.C. Wong, Z. Li, C.H. Tan, H. Zhong, Z. Huang, H. Bronstein, et al., Morphological stability and performance of polymer-fullerene solar cells under thermal stress: the impact of photoinduced PC60BM oligomerization, ACS Nano. 8 (2014) 1297–1308. http://dx.doi.org/10.1021/nn404687s (accessed 01.03.16).